

Intermediate asymptotics on crossover of scaling law on dynamical impact of viscoelastic surface

Hirokazu Maruoka¹

¹*Deep-Sea Nanoscience Research Group, Research Center for Bioscience and Nanoscience,
Research Institute for Marine Resource Utilization,
Japan Agency for Marine-Earth Science and Technology (JAMSTEC),
2-15 Natsushima-cho, Yokosuka, Kanagawa 237-0061, Japan**

(Dated: January 12, 2023)

In this Letter, a crossover of scaling laws is described as a result of the interference from self-similar variable of the higher class of the self-similarity on the dynamical impact of solid sphere onto a viscoelastic surface. All the physical factors including the size of spheres, the impact of velocity are successfully summarized to the primal dimensionless numbers which construct a self-similar solution of the second kind, which represents the balance between dimensionless numbers. The self-similar solution gives two different scaling laws by the perturbation method describing the crossover. These theoretical predictions are compared with experimental results to show good agreement. It was suggested that a hierarchical structure of similarity plays a fundamental role on crossover, which offers a fundamental insight to self-similarity in general.

Introduction.— “Scaling never appears by accident” [1]. Scaling law is the representation of physical law, which is expressed by a power-functional relation between physical parameters (e.g., Boyle’s law is the inverse-proportional relation between pressure and volume $P \sim V^{-1}$). It is quite general and basic concept in physics. It enable us to connect theory with experiment as theoretical verification is generally performed through the reference of the scaling relation obtained by the experimental observation [2]. On the other hand, one observes the case in which a scaling law transforms to another in different scale of physical variables, which we call *crossover* of scaling law, in a wide variety of fields: the mechanics of continua [3, 4], soft matter [5], quantum physics [6], critical phenomena [7, 8] and so on. Such phenomena are very interesting for application and biology as it is expected that they can be associated with the invention of functional materials [9, 10], and may play an important role on the biological functions [11–13]. Crossover of scaling laws can be formalized as *the process of transition of scaling law by the continuous change of a scale parameter*. However, the studies of crossovers generally focus on each scaling law in the extreme limit independently. As a result, they failed to formalize it as the continuous process.

The appearance of stable scaling law can be understood as an *intermediate asymptotic*, which is defined as an asymptotic representation of a function valid in a certain scale range [14–23]. Barenblatt has formalized the idealization of physical theory in terms of dimensional analysis. Dimensional analysis gives a self-similar solution of which variables are dimensionless numbers consisting of the physical quantities involved in the phenomena. If the dimensionless function converges to a finite limit, which corresponds to *complete similarity* [24], and that a single dimensionless number is remained, an intermediate asymptotic is obtained, which results in the scaling law which is *locally* valid in the range in which its

asymptotic is maintained. This formalization facilitates us to understand the idealization of physics and the dimensionless numbers though his theory is limited to the case of a single scaling law and has not developed to how crossovers are formalized.

In this Letter, I develop Barenblatt’s idea for crossover of scaling law. In terms of the concept of the intermediate asymptotic, it is expected that crossover must correspond to the case in which its idealization is broken. As previously mentioned, a single scaling law is obtained in the condition in which its dimensionless function converges to a finite limit. Conversely speaking, the incomplete convergence of dimensionless function, namely the interference of another dimensionless number may generate crossover of scaling law. I will demonstrate that we can understand crossover by such a framework; *crossover is generated by interference from another dimensionless number*.

To verify this framework, this work focuses on the contact mechanics [25, 26] in which crossovers of scaling laws are observed [27] depending on the form of contacts and the physical parameters can be easily controlled. The contact phenomena are abundant in our daily life [28, 29] and industry [30]. In the present work, I show the new scaling laws on the dynamical impact of the solid sphere onto the viscoelastic surface. The viscoelastic surface is quite interesting as it can be the model involving time-scale dependence, such as the earthquake [31]. The scaling relation between maximum deformation and the impact-velocity reveals a crossover depending on the impact-velocity and the size of spheres. I successfully integrate these elements into a single dimensionless number to find that the interference can be described by a self-similar solution of the second kind.

Maxwell viscoelastic foundation model.— Here we think about the problem in which a rigid sphere is free fall onto the viscoelastic surface (See Fig. 1). In this case, the

surface is modeled by the viscoelastic-foundation model in which the stress deformation is described by foundations which are arranged in parallel[32]. Each foundation consists of a dashpot (viscous coefficient μ) and a spring (elastic modulus E), which are serially connected. In this model, the stress σ and the deformation ϵ can be related by the following differential equation with time t , $\frac{\mu}{E} \frac{d\sigma}{dt} + \sigma = \mu \frac{d\epsilon}{dt}$, which corresponds to the Maxwell model. By assuming the deformation by the impact of sphere of which deformation is δ , thickness of surface is h , the contact area is a , the deformation at position from center of sphere r can be described by $\epsilon = \frac{\delta}{h} \left[1 - \left(\frac{r}{a} \right)^2 \right]$. Assuming the main contribution is due to $\frac{d\delta}{dt} \simeq \text{const}$ for the foundation, the energy of deformation is described by

$$E_{MVF} = \frac{\pi\mu\phi R\delta^2}{h} \frac{d\delta}{dt} \left[1 - \exp\left(-\frac{Et}{\mu}\right) \right] \quad (1)$$

where R is radius of sphere, ϕ is the fraction of contact and t is contact time.

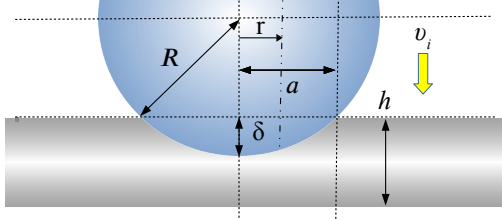


FIG. 1: (Color online) The geometrical parameters involved in the collision between elastic surface with its thickness h and solid sphere with its radius R in the impact-velocity v_i . The deformation δ and diameter of contact a are generated by the collision onto the viscoelastic surface. r is the position from center.

E_{MVF} is quite characteristic as it transforms depending on the contact time $\mu/Et = \text{De}$, Deborah number[33]. Supposing $\text{De} \gg 1$ which can be realized by the fast-time impact due to the following scaling $t_c \sim \delta_m/v_i$ where δ_m is maximum deformation, v_i is the impact-velocity and t_c is the contact time at which the deformation is maximized[34] and the relation of $\frac{d\delta}{dt} = v_i$, Taylor expansion is applied to E_{MVF} as follows; $E_{MVF} = \frac{\pi\mu\phi R\delta_m^2}{h} v_i \left[\frac{E\delta_m}{\mu v_i} - \dots \right] \simeq \frac{\pi E\phi R\delta_m^3}{h} = E_{el}$, which corresponds to the elastic energy[23, 35].

Suppose that the kinetic energy of the solid ball with the density ρ is converted to E_{MVF} , we have

$$\frac{2}{3}\pi R^3 \rho v_i^2 = \frac{\pi\mu\phi R\delta_m^2}{h} v_i \left[1 - \exp\left(-\frac{E\delta_m}{\mu v_i}\right) \right]; \quad (2)$$

it is energy conversion at which the deformation is maximized.

Dimensional analysis.— In order to see the self-similar structure, here I perform the dimensional

analysis[36]. The physical parameters which are involved are summarized to the following function $\delta_m = f(R, h, \phi, \rho, \mu, E, v_i)$. The dimensions of the function is described as follows; $[\delta_m] = L, [R] = L, [h] = L, [\phi] = 1, [\rho] = M/L^3, [\mu] = M/LT, [E] = M/LT^2, [v_i] = L/T$ by LMT unit. By selecting R, ρ, v_i as the governing parameters with independent dimensions, which are defined as the parameters which cannot be represented as a product of the remaining parameters, following self-similar variables are defined:

$$\Pi = \frac{\delta_m}{R}, \quad \kappa = \frac{h}{R}, \quad \eta = \frac{\rho v_i^2}{E}, \quad \theta = \frac{\mu}{E^{1/2} \rho^{1/2} R} \quad (3)$$

then we have $\Pi = \Phi(\phi, \kappa, \theta, \eta)$ where η corresponds to Cauchy number, dimensionless velocity-component. To know the self-similar structure, here I check the convergence of the dimensionless function. In the short time contact, we have the elastic energy then we have the solution,

$$\Pi = \text{const} \left(\frac{\kappa}{\phi} \right)^{\frac{1}{3}} \eta^{\frac{1}{3}} \quad (4)$$

which corresponds to Chastel-Gondret-Mongruel (CGM) solution[35, 37, 38]. We easily find that Φ does not converge as η goes to infinity according to Eq. (4), which means that Φ is incomplete similarity (see Ref. [24]). However, we can make it converge by defining another self-similar variables as follows, $\Psi = \frac{\Pi^3 \phi}{\kappa \eta}$ for $\Psi = \text{const}$ as $\eta \rightarrow \infty$. Thus Ψ construct a self-similarity of different class, which corresponds to the self-similarity of the second kind[40]. By considering these structure and applying these self-similar variables into Eq. (3), one finds that the similarity can be complete if we construct another self-similar variables as $Z = \frac{\Pi}{\theta \eta^{1/2}} = \frac{E\delta_m}{\mu v_i}$ then we have

$$\Psi = \frac{2}{3} \frac{Z}{[1 - \exp(-Z)]}. \quad (5)$$

Supposing $\Psi = \Phi(Z)$, Φ converges to a finite limite as Z goes to zero[39]. Therefore, equation (5) belongs to a self-similar solution of the second kind, which is defined as the power-exponents of self-similar variables cannot be determined by dimensional analysis and mathematically corresponds to a *fractal*[41].

Note that there is a hierarchical structure on the self-similar solution in Eq. (5) depending on the convergence of dimensionless function (See Fig. S2). $\Pi, \kappa, \theta, \phi$ and η belong to a similarity-class which forms a following similarity structure: $\frac{\Pi^3 \phi}{\kappa \eta} = \Phi\left(\frac{\Pi}{\theta \eta^{1/2}}\right)$. Here I call this class similarity of *the first class* as it is generated through dimensional analysis. In the first class, each parameters belong to dimensionless physical quantities. On the other hand, Ψ and Z belong to an another similarity-class to form the following similarity structure: $\Psi = \Phi(Z)$. I

call this class similarity of *the second class*[42]. The variables of the second class normalizes the difference of the variables of the first class to integrate the single lines, which corresponds to the data collapse[43, 44]. In the second class, self-similar variables represents the dynamics of energy involved in the process. Ψ represents the proportion of kinetic energy and elastic energy while Z represents the proportion of viscous energy and elastic energy, which corresponds to Deborah number. One can find that $\Phi(Z)$ represents the interference of viscous components. If Z goes to 0, which can be achieved by the high-velocity impact or short-time contact, $\Phi \rightarrow \text{const}$, then we have the CGM solution, which is realized in the case in which the kinetic energy fully transforms to elastic energy. Here the convergence of $\Phi(Z)$ means the inactiveness of Z . Thus in case of $Z \ll 1$, the impact is elastically dominant, which we call elastic impact and it gives 1/3 power-law on η . However, when this idealized condition is not satisfied ($Z > 1$), which can be realized by the low-velocity impact, the viscous components $\Phi(Z)$ interferes Ψ . In this region, the viscosity contributes in the impact, then it changes scaling law. This impact corresponds to the viscoelastic impact.

We cannot see the actual scaling behavior of Π and η in viscoelastic regime from the second class. They belong to the first class and their behaviors are not simply consistent with Ψ and Z as one see $\frac{\Pi^3 \phi}{\kappa \eta} = \Phi\left(\frac{\Pi}{\theta \eta^{1/2}}\right)$, which shows that Π and η are included in both variables of the higher class, Ψ and Z . In order to know the scaling-behavior of Π and η , here I apply the third term perturbation method, then we have

$$\Pi = \frac{\kappa}{54\phi\theta^2} + \left(\frac{\kappa^2}{486\phi^2\theta^3}\right)^{\frac{1}{3}} \eta^{\frac{1}{6}} + \left(\frac{2\kappa}{3\phi}\right)^{\frac{1}{3}} \eta^{\frac{1}{3}} \quad (6)$$

as $\varepsilon = \frac{1}{\theta \eta^{1/2}} \rightarrow 0$ [45].

As we can see, Eq. (6) includes two different power exponents as $\eta^{1/3}$ and $\eta^{1/6}$, which suggests that intermediate asymptotics appear depending on θ , η or Z . In case of the impact of high velocity and/or smaller sphere, which corresponds to $\eta \gg 1$ and/or $\theta \gg 1$ and $Z \ll 1$, $\eta^{1/3}$ is dominant. Conversely in the region of viscoelastic impact in which $Z > 1$, realized by low-velocity $\eta \ll 1$ and/or the impact of larger sphere $\theta \ll 1$, $\eta^{1/6}$ is dominant while the intermediate behavior may be realized in $Z \sim 1$.

Experiment.— To show the validity of the theory, the experiments have been performed using a viscoelastic surface made of polydimethylsiloxane (PDMS), of which thickness $h = 7.5$ mm, $\phi = 1$, elastic modulus $E \simeq 0.57$ MPa and viscous coefficient $\mu = 117$ kPa · s. The PDMS surface was coated with grease to prevent the adhesive effect. The metallic ball was suspended by the electromagnet of which magnet force is controlled (Fig. S3). The ball is dropped onto the PDMS surface and the collision is observed by high speed camera (Fig. S4). The

size of sphere R is differed as 3.0, 4.0, 5.0, 6.0, 7.0 and 8.0 mm, of which density $\rho = 7800$ kg · m⁻³. The physical parameters were extracted by image analysis. Using these numerical estimations, the dimensionless numbers of the self-similarity of the first class, and the second class were calculated[46].

Figure 2 shows the self-similar variables in different self-similarity class. Figure 2 (a - f) demonstrates the self-similarity of the first class, which is the power-law relation between Π and η in different size of spheres while Figure 2 (g) demonstrates the self-similarity of the second class, which is their Ψ and Z . As we can see, the plots of Π and η reveal gradually different scaling law from $R = 3.0$ mm to 8.0 mm.

Equation (6) predicts that Π and η have different power law depending on θ and η , finally summarized to $\Phi(Z)$. As the prediction mentioned in previous section suggests, the impacts of the smaller spheres ($R = 3.0, 4.0$ mm) which tends to have smaller Z follow 1/3 power-law, which corresponds to elastic impact (Fig. 2 (a, b)). $\Phi(Z)$ belonging to the plots of 1/3 power-law shows the smaller Z and tendency to convergence to a finite limit, which signifies that $\Phi(Z)$, viscous component hardly contribute. On the other hand, larger spheres ($R = 7.0, 8.0$ mm) reveal different power-law, which is closer to 1/6 power-law in low-velocity (Fig. 2 (e, f)). The plots revealing 1/6 power-laws belong to the larger Z and Ψ increases in Fig. 2 (g), which means that viscous component $\Phi(Z)$ contributes and it is viscoelastic impacts. The dash-dots lines which are described by Eq. (6) are consistent with the power-law behavior of the plots. The plots of intermediate size of spheres ($R = 5.0, 6.0$ mm) reveals slightly intermediate scaling law between 1/3 and 1/6 though this behavior is well described by the Eq. (6). All these plots roughly follow the line described by the self-similar solution of Eq. (5) in Fig. 2 (g).

The deviation of plots from the theoretical lines may be originated from the technical reason and the theoretical assumption. The adhesion effect was decreased by coating grease though it may depend on the size of spheres. The model assumes the main contribution is due to $\frac{d\delta}{dt} = \text{const}$ while the velocity steeply decreases in the end. Thus, experimentally the coefficient between t_c and δ_m/v_i is found then we used a following relation on the calculation ; $1/\text{De} \simeq 1.90Z$. However, these effect did not change the scaling relation and was only reflected on the coefficient (See Fig. 5S). Furthermore, the foundation model considers only vertical deformation though it is not completely satisfied actually, which might make difference. Despite these considerations, we can say that the scaling behaviors were well described by theoretical lines, which demonstrates the good consistency.

Discussion.— The analysis based on the different class of self-similarity gives different view of the process. The scaling behavior of the first class, which is apparent to our interest, is not clear within this class as the actual

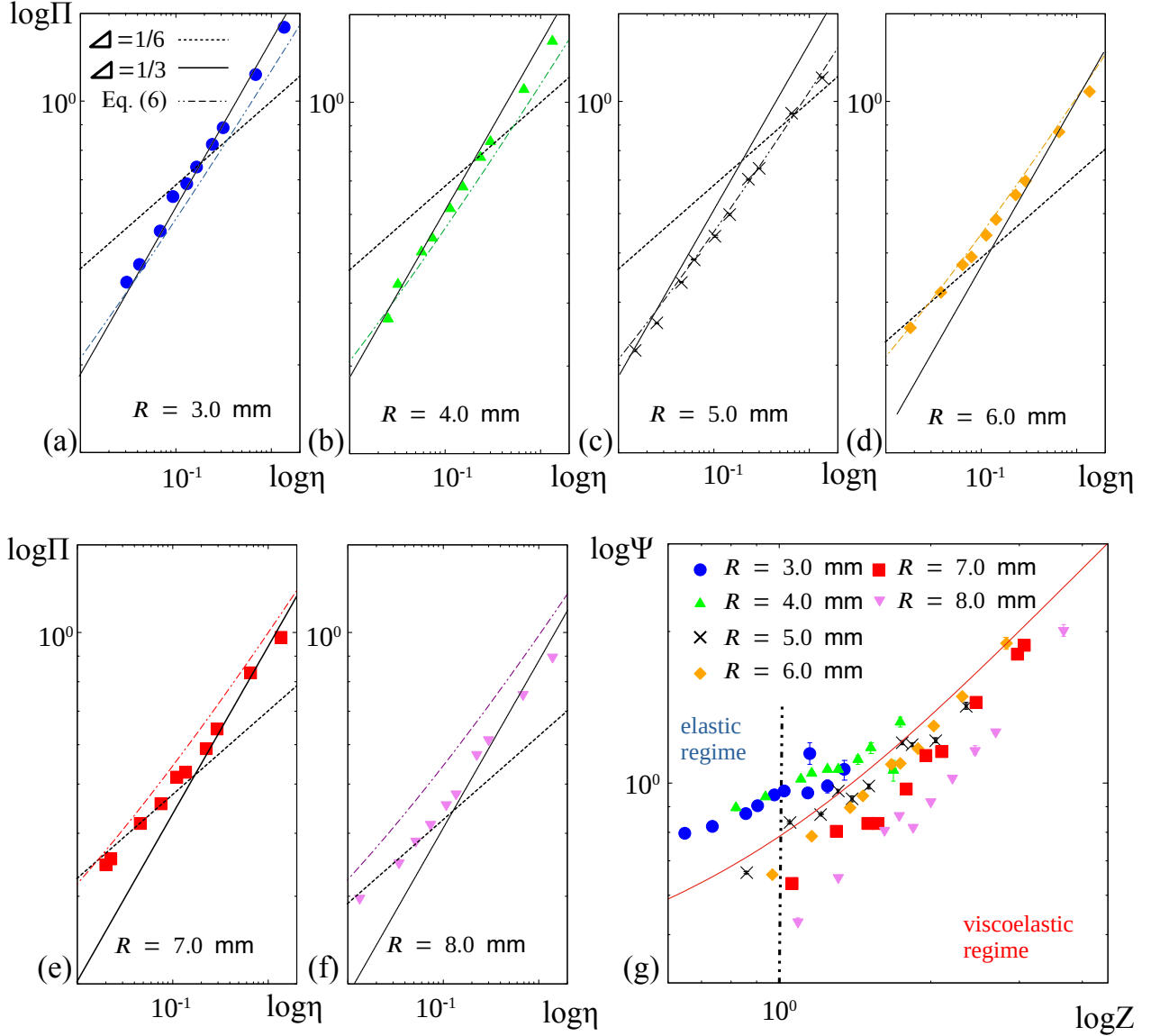


FIG. 2: (Color online) The different hierarchical structure of self-similarity. (a) - (f) Self-similarity of the first class : the power law relations Π and η in different size of sphere. The dashed lines indicates the slope of $1/6$, the solid line indicates the slope of $1/3$ and colored dot-dashed line indicates Eq. (6) in each size of spheres. (g) Self-similarity of the second class : the plots between Ψ and Z . $R = 3.0$ mm (\bullet), 4.0 mm (\blacktriangle), 5.0 mm (\times), 6.0 mm (\blacklozenge), 7.0 mm (\blacksquare) and 8.0 mm (\blacktriangledown) where $\Pi = \delta_m/R$, $\eta = \rho v_i^2/E$, $\Psi = \frac{\Pi^3 \phi}{\kappa \eta} = \frac{\delta_m^3 E}{R^2 \hbar \rho v_i}$ and $Z = \frac{\Pi}{\theta \eta^{1/2}} = \frac{E \delta_m}{\mu v_i}$. The red line in Figure (g) is Eq. (5).

behavior of the scaling laws are finally determined by the competition of the self-similar variables of the second class, which is expressed as the self-similar solution : $\Psi = \Phi(Z)$. Therefore, the transition of the scaling law, which corresponds to crossover, cannot be explained without the consideration of this hierarchical structure. $\Phi(Z)$ does not only qualitatively decide the crossover but also it numerically expresses the balance between the di-

dimensionless numbers. This numerical balance accurately decides the balance of coefficients of Eq. (6), which enables us to describe the exact behaviors of crossover more accurately.

It is expected that the framework which was shown in this Letter is not limited to this present work. All the stable scaling laws should be intermediate asymptotics in which dimensionless functions converge. Thus the tran-

sition of scaling laws must be given by the violation of this idealization. Yasuda et al. also reported the primal dimensional number to change the scaling laws[47]. Barenblatt reported the dependence of power exponents by another dimensionless numbers[48, 49] though in these cases the exact form of dimensionless function Φ were unclear and the hierarchy was not focused on. In the present work, I succeeded to identify the exact form of dimensionless functions. The insights in the present work suggested that the investigation of hierarchy of the higher class can be the clue to describe crossover.

Conclusion.— The above discussion with experimental results confirms the validity of Eq. (5) with Eq. (6) as the fundamental equation of this problems. In this Letter, I have succeeded to demonstrate that the *crossover of scaling is generated by the interference of the self-similar variables of the higher class*, which corresponds to the framework mentioned in the introduction. The method exercised in this work is unique in terms of methodology as the degree of this interference is quantitatively and qualitatively estimated and it enable us to describe crossover as the continuous process more accurately.

Finally, intermediate asymptotics is the *locally* valid asymptotic expression while we have found that this locality is governed by the self-similar solution of the higher class in this Letter. This framework is simple and expected to be quite general in physics. Besides, it is similar to critical phenomena in which the transition of phase is generated by the continuous parameter variation. Therefore, the present work supplies interesting insights for the concept of self-similarity, nonequilibrium theory and critical phenomena, for a wide variety of fields in physics in general.

Acknowledgement.—The author wishes to thank D. Nishiura for technical assistance of the experiments, G. Li for technical advice of experimental setup, D. Matsuoka for technical advice for the algorithm of the program for image analysis, S. Okada, E. Barbieri and Y. Kawamura for helpful discussion and many support for the experiment. He is appreciated with the members at MAT (Center for Mathematical Science and Advanced Technology) seminar at JAMSTEC for fruitful discussion.

* Electronic address: maruokah@jamstec.go.jp; Electronic address: hmaruoka1987@gmail.com

- [1] G. I. Barenblatt, *Scaling* (Cambridge University Press, 2003) p.1.
- [2] P.-G. de Gennes, *Scaling Concepts in Polymer Physics* (Cornell University Press, 1979).
- [3] M. Yokota, K. Okumura, Dimensional crossover in the coalescence dynamics of viscous drops confined in between two plates, Proc. US Nat. Acad. Sci. **108**, 6395 (2011).
- [4] M. Murano and K. Okumura, Rising bubble in a cell with a high aspect ratio cross-section filled with a viscous fluid and its connection to viscous fingering, Phys.Rev.Res., **2**, 013188 (2020).
- [5] G. C. Berry and T. G. Fox, The Viscosity of Polymers and Their Concentrated Solutions, Adv. Polym. Sci. **5**, 261 (1968).
- [6] R. Vasseur, K. Trinh, S. Haas, and H. Saleur, Crossover Physics in the Nonequilibrium Dynamics of Quenched Quantum Impurity Systems, Phys. Rev. Lett. **110**, 240601 (2013).
- [7] E. Lujiten and H. W. J. Blöte, Crossover scaling in two dimensions, Phys. Rev. E **56**, 6540 (1997).
- [8] S. Lübeck, Universal Behavior of Crossover Scaling Functions for Continuous Phase Transitions, Phys.Rev.Lett., **90**, 210601 (2003).
- [9] W. J. Parnell and R. De Pascalis, Soft metamaterials with dynamic viscoelastic functionality tuned by pre-deformation, Phil. Trans. R. Soc. A, **377**: 20180072, (2019).
- [10] R. N. Glaesener, J.-H. Bastek, F. Gonon, V. Kannan, B. Telgen, B. Spöttling, S. Steiner, D. M. Kochmann, Viscoelastic truss metamaterials as time-dependent generalized continua, J. Mech. Phys. Solids., **156** 104569, (2021).
- [11] The discontinuous transition of biological function by the change of physical parameters are discussed as "Funktionswandel" in the following book: V. v. Weizsäcker, *Der Gestaltkreis. Theorie der Einheit von Wahrnehmen und Bewegen* (Suhrkamp, 1997).
- [12] B. Bhushan, Biomimetics: lessons from nature — an overview, Phil. Trans. R. Soc., **367** 1445, (2009).
- [13] U. Krohs, The Epistemology Biomimetics: The Role of Models and of Morphogenetic Principles, Perspective on Science, **29** 583, (2021).
- [14] See Supplemental Material for Intermediate asymptotics.
- [15] See Ref. [1] pp.60 - 65.
- [16] G. I. Barenblatt, *Scaling, self-similarity, and intermediate asymptotics* (Cambridge University Press, 1996) pp.86-94.
- [17] G. I. Barenblatt, *Flow, Deformation and Fracture* (Cambridge University Press, 2014).
- [18] G. I. Barenblatt and Ya. B. Zeldovich, Self-similar solutions as intermediate asymptotics, Ann. Rev. Fluid Mech. **4**, 285 (1972).
- [19] N. Goldenfeld, O. Martin and Y. Oono, Intermediate asymptotics and renormalization group theory, J. Sci. Comput. **4**, 355 (1989).
- [20] N. Goldenfeld, *Lecture On Phase Transitions And The Renormalization Group* (Addison-Wesley Publishing Company, 1992) Ch.10.
- [21] M. Benzaquen, T. Salez, E. Raphaël, Intermediate asymptotics of the capillary-driven thin-film equation, Eur. Phys. J. E **36** 82, (2013).
- [22] O. Bäumchen, M. Benzaquen, T. Salez, J. D. McGraw, M. Backholm, P. Fowler, E. Raphaël, K. D.-Veress, Relaxation and intermediate asymptotics of a rectangular trench in a viscous film, Phys.Rev.E **88**, 035001 (2013).
- [23] H. Maruoka, Intermediate asymptotics on dynamical impact of solid sphere on mili-textured surface, Phys.Rev.E **100**, 053004 (2019).
- [24] See Refs. [1] (pp. 82-87), [16] (pp. 145-160) and [17] (pp. 153-163). The case in which dimensionless function obtained by dimensional analysis $\Phi(\xi, \eta)$ converges to a finite limit as $\xi \rightarrow 0$ or ∞ corresponds to *complete similar-*

- ity* or *similarity of the first kind* in ξ while the case in which the complete similarity is not satisfied but the convergence of dimensionless function is recovered by constructing the new self-similar variables as Π/η^ζ and ξ/η^ϵ , corresponds to *incomplete similarity* or *similarity of the second kind*. See Supplemental Material for Complete similarity and incomplete similarity.
- [25] H. Hertz, *Miscellaneous Papers* (MacMillan & CO, 1896) p 146.
- [26] K. L. Johnson, *Contact mechanics* (Cambridge University Press, 1985).
- [27] L. Kogut and I. Etsion, Elastic-Plastic Contact Analysis of a Sphere and a Rigid Flat, *J. Appl. Mech.* **69**, 657 (2002).
- [28] R. W. Carpick, Approximate models of interacting surfaces competed against a supercomputer solution, *Science* **359**, 38 (2018).
- [29] A. M. Nathan, J. J. Crisco, R. M. Greenwald, D. A. Russell and L. V. Smith, A comparative study of baseball bat performance, *Sports Eng.* **13**, 153 (2011).
- [30] I. G. Goryacheva, *Contact Mechanics in Tribology* (Kluwer Academic Publishers, 1998).
- [31] H. Suito, Importance of rheological heterogeneity for interpreting viscoelastic relaxation caused by the 2011 Tohoku-Oki earthquake, *Earth, Planets and Space* **69**:21 (2017).
- [32] See Ref. [26] (pp.104-106).
- [33] M. Reiner, The Deborah Number, *Physics Today* **17**, 62 (1964).
- [34] See Ref. [26] p. 353.
- [35] T. Chastel, P. Gondret and A. Mongruel, Texture-driven elasto-hydrodynamic bouncing, *J.Fluid Mech.* **805**, 577 (2016).
- [36] See Refs. [1] (pp. 91-93), [16] (pp.159-160).
- [37] T. Chastel and A. Mongruel, Sticking collision between a sphere and a textured wall in a viscous fluid, *Phys. Rev. Fluids* **4**, 014301 (2019).
- [38] A. Mongruel and P. Gondret, Viscous dissipation in the collision between a sphere and a textured wall, *J. Fluid Mech.* **896** (2020).
- [39] $\Phi(Z)$ looks like a indeterminate form as $Z \rightarrow 0$ though the convergence can easily be verified by L'Hôpital's rule. See Supplemental Material for The convergence of Eq. (5).
- [40] See Refs. [1] (pp.82-91), [16] (pp.151-159) and [17] (pp. 153-163). See Supplemental Material for Complete similarity and incomplete similarity.
- [41] B. B. Mandelbrot, *The fractal geometry of nature* (Macmillan, 1983).
- [42] Barenblatt formulated the category for the first kind and the second kind as the property of convergence of dimensionless function. However, one can note that there exists a hierarchy of the class to which physical quantities belong, the class to which dimensionless parameters composed by dimensional analysis belong and the class to which dimensionless parameters which is power-law monomial of dimensionless parameters to recover the convergence belong. In order to refer these classes depending on which kind of parameters belong, here I invent the terms *the first class* and *the second class*. See Supplemental Material for The hierarchical structure of self-similarity and Fig. 2S.
- [43] S. M. Bhattacharjee and Flavio Seno, A measure of data collapse for scaling, *J. Phys. A: Math. Gen.* **34** 6375, (2001).
- [44] H. Nakazato, Y. Yamagishi and K. Okumura, Self-similar dynamic of air film entrained by a solid disk in confined space: A simple prototype of topological transitions, *Phys.Rev.Fluid*, **3**, 054004 (2018).
- [45] See Supplemental Material for the derivation of Eq. (6).
- [46] See Supplemental Material for The detailed of the Experiment. See Supplemental Material at [] for a movie of a dynamical impact of solid sphere ($R = 6$ mm) onto the viscoelastic surface at $v_i = 370$ mm/s with the frame rate for 10000 image per second and the resolution of 768×768 pixels.
- [47] T. Yaduda, N. Sakumichi, U. Cheng, T. Sakai, Universal Equation of State Describes Osmotic Pressure throughout Gelation Process, *Phys.Rev.Lett.* **125**, 267801 (2020).
- [48] G. I. Barenblatt, A. J. Chorin and V. M. Prostokishin, A model of a turbulent boundary layer with a nonzero pressure gradient, *Proc. US Nat. Acad. Sci.* **99**, 5572 (2002).
- [49] G. I. Barenblatt and L. R. Botvina, Incomplete similarity of fatigue in a linear range of crack growth, *Fatigue Eng. Mater. Struct.* **3**, 193 (1981).

Supplemental materials to the manuscript of Intermediate asymptotics on crossover of scaling law on dynamical impact of viscoelastic surface

INTERMEDIATE ASYMPTOTICS

In this section, I briefly explain the concept of *intermediate asymptotics* which is formalized by Barenblatt[1–4] by using a simple example. Intermediate asymptotics is an asymptotic representation of a function valid in a certain range of independent variables, which corresponds to a kind of the formalization of the idealization which accompanies with the construction of physical model. To understand this concept, the following problem of dimensional analysis might be helpful. Imagine that the circle is pictured on the surface of the sphere (See Fig. S1). In this problem, the physical parameters that are involved are the surface area of circle S , radius of the circle r and the radius of sphere R . Here we would like to know the scaling behavior between S and r . Therefore we have the functional relation as follows: $S = f(r, R)$.

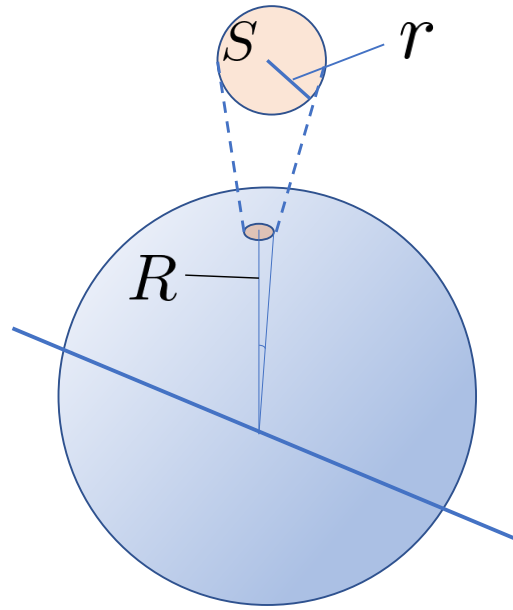


FIG. S1: (Color online) A circle of which radius is r and surface area is S , described on a sphere of which radius is R .

According to dimensional analysis, as the dimension of physical parameters $[S] = L^2$, $[r] = L$ and $[R] = L$, selecting r as a governing parameter of independent dimension, we have the following dimensionless function,

$$\Pi = \Phi(\theta) \quad (S1)$$

where $\Pi = \frac{S}{r^2}$ and $\theta = \frac{r}{R}$.

By the geometrical consideration, we have the exact form of Φ as follows,

$$\Phi(\theta) = 2\pi \frac{1 - \cos\theta}{\theta^2}. \quad (S2)$$

To know the behavior of Φ in the case in which $\theta \rightarrow 0$, which corresponds to the increase of R or the decrease of r , Taylor expansion is applied to Eq. (S2) then we have,

$$\Pi = \Phi(\theta) \simeq \pi - \frac{\pi}{12}\theta^2 \cdots + \xrightarrow{\theta \rightarrow 0} \pi. \quad (S3)$$

As Eq. (S3) shows, Φ converges to a finite limit π , then we have a following intermediate asymptotics as $\Pi = \frac{S}{r^2}$,

$$S = \pi r^2 \quad (0 < r \ll R) \quad (S4)$$

as far as the asymptotic condition $\theta \ll 1$, corresponding to $0 < r \ll R$, is satisfied.

Note that the scaling law Eq. (S4) is valid in the scale range ($0 < r \ll R$), in which the circle is significantly smaller than the sphere. Therefore, Eq. (S4) is an asymptotic expression which is valid in the certain range of variable r . This scaling law formalized *locally* is an intermediate asymptotic in this problem.

The important point of this concept is that every physical problem has dimension and can be applied dimensional analysis to obtain dimensionless function Φ . By considering the convergence of Φ , some self-similar variables can be selected to have the idealized solution effectively and practically as the convergence of Φ can be verified by the experimental or simulation results even if the exact form of Φ is not obtained. This procedure give rise to the strategy of Barenblatt as it is formalized in the recipe[5].

The second important point is that this process, in which screening the self-similar variables of Φ depending on their convergence, corresponds to the idealization of the problems. More or less, all the physical models involve the idealization such as ignorance of friction force, ignorance of quantum or relativity effect. All these assumption corresponds to the idealizing process of dimensionless function. For example, ideal gas equation can be considered as an intermediate asymptotic valid in the range where the volume of molecules b and the molecular interaction a are negligible on van der Waals equation as follows,

$$p = \frac{nRT}{V - nb} - \frac{an^2}{V^2} \rightarrow \frac{nRT}{V} \left(\frac{an^2}{V^2} \ll p \ll \frac{RT}{b} \right). \quad (\text{S5})$$

This idealizing scale range is satisfied as far as $\Pi_a = \frac{an^2}{pV^2} \ll 1$ and $\Pi_b = \frac{pb}{RT} \ll 1$.

This concept suggests that every physical theory is *locally* valid. This localization is quantitatively and qualitatively formalized by the intermediate asymptotics. In the present work, the author focuses on this point and consider the case of the transition of this *locality*.

COMPLETE SIMILARITY AND INCOMPLETE SIMILARITY

In this section, I briefly explain *complete similarity* and *incomplete similarity*, as well as the *self-similarity of the first kind* and the *self-similarity of the second kind* [6]. They are the category in terms of the convergence of dimensionless function. Zeldovich noted that there exists the type of self-similarity[7]. As the previous section showed, the self-similar solution is obtained by dimensional analysis. Supposing that a certain physical function,

$$y = f(t, x, z) \quad (\text{S6})$$

in which y , t , x and z are certain physical quantities which have physical dimensions. Selecting t as a governing parameter with independent dimension, which is defined as physical parameters which cannot be represented as a product of the remaining parameters, then we apply dimensional analysis to have

$$\Pi = \Phi(\eta, \xi) \quad (\text{S7})$$

where $\Pi = y/t^\alpha$, $\eta = x/t^\beta$ and $\xi = z/t^\gamma$. α , β and γ are determined by the dimension of parameters through dimensional analysis.

If Φ converges to a finite limit as ξ goes to zero or infinity, this case corresponds to *complete similarity* or *similarity of the first kind* in the similarity parameter ξ . In this case, ξ can be excluded on the consideration and we have an intermediate asymptotics. Once η and ξ both satisfy the complete similarity then $\Phi \rightarrow \text{const}$ as $\eta \ll 1$ and $\xi \ll 1$, then we have a following intermediate asymptotic, $y = \text{const } t^\alpha$ ($0 < t \ll x^{1/\beta}$, $0 < t \ll z^{1/\gamma}$). When the self-similar variables satisfies the condition of complete similarity, $\Pi = \Phi(\xi, \eta)$ is corresponds to a *self-similar solution of the first kind*. In the previous section, as Eq. (S3) shows, the dimensionless function converges to a finite limit, therefore the problem belongs to complete similarity and Eq. (S1) is a self-similar solution of the first kind.

On the other hand, in the case in which the complete similarity is not satisfied, namely Φ does not converge to a finite limit as η goes to zero or infinity, but the convergence is recovered by constructing new self-similar variables as the power-law monomial using dimensionless variables, this case corresponds to *incomplete similarity* or *similarity of the second kind*. In this case, we may have the following self-similar solution, which is called *self-similar solution of the second kind*,

$$\Psi = \Phi(Z) \quad (\text{S8})$$

where $\Psi = \Pi/\eta^\zeta$ and $Z = \xi/\eta^\epsilon$.

The first important point is that the power exponent ζ and ϵ cannot be determined by dimensional analysis in case of the second kind while it is possible in case of the first kind. We may occasionally determine ζ and ϵ by the method for nonlinear eigenvalue problems[8] or renormalization group theory [9, 10] though we may consider them as simply empirical numbers[11].

The second important point is that there exists hierarchy of self-similarity. Note that we can find a parallelism between the first kind and the second kind. Dimensional analysis transforms $y = f(t, x, z)$ to $y/t^\alpha = \Phi(x/t^\beta, z/t^\gamma)$ while $\Pi = \Phi(\eta, \xi)$ is transformed to $\Pi/\eta^\zeta = \Phi(\xi/\eta^\epsilon)$ in case of the second kind.

Barenblatt formalized the type of the self-similarity depending on the convergence of dimensionless function. He insisted that all the theory can be deduced to the self-similar solution.

THE HIERARCHICAL STRUCTURE OF SELF-SIMILARITY

As the previous section suggested, the hierarchy on self-similarity is found. However, Barenblatt utilizes the similarity of the first kind or the second kind for the property of the self-similar solution. In my work, I came to realize that the hierarchy of self-similarity is important as the interference of dimensionless number is finally expressed by the self-similar solution of the higher class. Thus I invent the term referring the hierarchical class of the self-similarity. I defined the class which are constructed by dimensional analysis as self-similarity of *the first class* and the class which are constructed via the similarity parameters of the second kind as the self-similarity of *the second class*. Fig. S2 shows the hierarchy of self-similarity on the dynamical impact of solid sphere onto the viscoelastic surface.

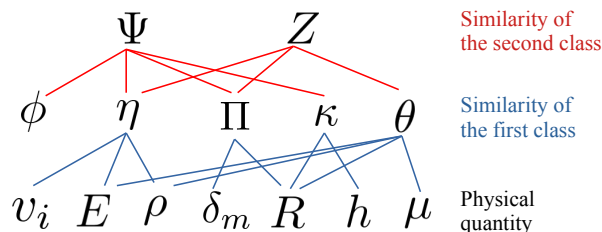


FIG. S2: (Color online) The hierarchy of self-similarity on the dynamical impact of solid sphere onto the viscoelastic surface. The solid lines signifies the composition of each dimensionless parameters. In the present study, one finds that there is a hierarchy on self-similar variables ; the class to which physical quantities belong, the class to which dimensionless parameters composed by dimensional analysis belong and the class to which dimensionless parameters which is power-law monomial of dimensionless parameters to recover the convergence belong.

THE CONVERGENCE OF EQ. (5).

Eq. (5) is seemingly a indeterminate form as $Z \rightarrow 0$ though it converges to a finite limit as follows. Using L'Hôpital's rule, then we have

$$\lim_{Z \rightarrow 0} \frac{2}{3} \frac{Z}{1 - e^{-Z}} = \lim_{Z \rightarrow 0} \frac{2}{3} \frac{(Z)'}{(1 - e^{-Z})'} = \frac{2}{3}. \quad (\text{S9})$$

THE DERIVATION OF EQ. (6)

According to Eq. (4), in the self-similarity of the first class, we have

$$\frac{\Pi^3 \phi}{\kappa \eta} = \frac{2}{3} \frac{\frac{\Pi}{\theta \eta^{1/2}}}{\left[1 - \exp\left(-\frac{\Pi}{\theta \eta^{1/2}}\right)\right]}. \quad (\text{S10})$$

By multiplying $\frac{\kappa\eta}{\Pi^3\phi}$ and we have the following form from Eq. (S10)

$$\frac{2}{3} = \Pi^2\theta\frac{\phi}{\kappa}\frac{1}{\eta^{1/2}} \left[1 - \exp\left(-\frac{\Pi}{\theta\eta^{1/2}}\right) \right]. \quad (\text{S11})$$

In order to see the actual behavior of Π , I applied the third term perturbation method. As it belongs to the problem of the singular perturbation[12], therefore here we assume

$$\Pi = \frac{1}{\varepsilon^\gamma} (\Pi_0 + \varepsilon^\alpha\Pi_1 + \varepsilon^{2\alpha}\Pi_2 + \dots) \quad (\text{S12})$$

where γ and α are constant, $\varepsilon = 1/\theta\eta^{1/2}$.

By applying the Taylor expansion on the exponential part and substituting Eq. (S12) into Eq. (S11), we have

$$\begin{aligned} & \theta^2\frac{\phi}{\kappa}\varepsilon\Pi^2 \left\{ \varepsilon\Pi - \frac{1}{2}\varepsilon^2\Pi^2 + \frac{1}{6}\varepsilon^3\Pi^3 \dots \right\} = \frac{2}{3} \\ \Leftrightarrow & \theta^2\frac{\phi}{\kappa}\varepsilon^{1-2\gamma} (\Pi_0^2 + 2\varepsilon^\alpha\Pi_1\Pi_0 + 2\varepsilon^{2\alpha}\Pi_2\Pi_0 + 2\varepsilon^{2\alpha}\Pi_1^2 + \dots) \{ \varepsilon^{1-\gamma} (\Pi_0 + \varepsilon^\alpha\Pi_1 + \varepsilon^{2\alpha}\Pi_2 + \dots) \\ & - \frac{1}{2}\varepsilon^{2-2\gamma} (\Pi_0^2 + 2\varepsilon^\alpha\Pi_1\Pi_0 + 2\varepsilon^{2\alpha}\Pi_2\Pi_0 + 2\varepsilon^{2\alpha}\Pi_1^2 + \dots) + \frac{1}{6}\varepsilon^{3-3\gamma} (\Pi_0^3 \dots) \dots \} = \frac{2}{3} \end{aligned} \quad (\text{S13})$$

as $\varepsilon \rightarrow 0$.

To balance each terms, we find that $\gamma = 2/3$ and $\alpha = 1/3$ then we obtain,

$$\begin{aligned} & \theta^2\frac{\phi}{\kappa} (\Pi_0^2 + 2\varepsilon^{1/3}\Pi_1\Pi_0 + 2\varepsilon^{2/3}\Pi_2\Pi_0 + 2\varepsilon^{2/3}\Pi_1^2 + \dots) \{ \Pi_0 + \varepsilon^{1/3}\Pi_1 + \varepsilon^{2/3}\Pi_2 + \dots \\ & - \frac{1}{2}\varepsilon^{1/3} (\Pi_0^2 + 2\varepsilon^{1/3}\Pi_1\Pi_0 + 2\varepsilon^{2/3}\Pi_2\Pi_0 + 2\varepsilon^{2/3}\Pi_1^2 + \dots) + \frac{1}{6}\varepsilon^{2/3} (\Pi_0^3 \dots) \dots \} = \frac{2}{3}. \end{aligned} \quad (\text{S14})$$

From this we have

$$\begin{aligned} O(1) \Leftrightarrow & \theta^2\frac{\phi}{\kappa}\Pi_0^3 = \frac{2}{3} \\ \Pi_0 & = \left(\frac{2}{3}\right)^{\frac{1}{3}} \frac{1}{\theta^{2/3}} \left(\frac{\kappa}{\phi}\right)^{\frac{1}{3}} \end{aligned} \quad (\text{S15})$$

$$\begin{aligned} O(\varepsilon^{1/3}) \Leftrightarrow & 3\Pi_0^2\Pi_1 - \frac{1}{2}\Pi_0^4 = 0 \\ \Pi_1 & = \frac{1}{6}\Pi_0^2 = \frac{1}{\theta^{4/3}} \left(\frac{\kappa}{\phi}\right)^{\frac{2}{3}} \left(\frac{1}{486}\right)^{\frac{1}{3}} \end{aligned} \quad (\text{S16})$$

$$\begin{aligned} O(\varepsilon^{2/3}) \Leftrightarrow & 3\Pi_0^2\Pi_2 - 2\Pi_0^3\Pi_1 + \frac{1}{6}\Pi_0^5 + 3\Pi_0\Pi_1^2 = 0 \\ \Pi_2 & = \frac{2}{3}\Pi_0\Pi_1 - \frac{1}{18}\Pi_0^3 - \frac{\Pi_1^2}{\Pi_0} = \frac{1}{54\theta^2} \frac{\kappa}{\phi} \end{aligned} \quad (\text{S17})$$

Using results of Eq. (S15), Eq. (S16), Eq. (S17), $\gamma = 2/3$ and $\alpha = 1/3$ for Eq. (S12) then we have a following result,

$$\Pi = \frac{\kappa}{54\phi\theta^2} + \left(\frac{\kappa^2}{486\phi^2\theta^3}\right)^{\frac{1}{3}} \eta^{\frac{1}{6}} + \left(\frac{2\kappa}{3\phi}\right)^{\frac{1}{3}} \eta^{\frac{1}{3}} \quad (\text{S18})$$

which corresponds to the Eq. (6).

THE DETAILED INFORMATION OF EXPERIMENT

The experimental setup was sketched in Fig. S3. The polydimethylsiloxane (PDMS) (SILPOT™ 184 W/C, DOW) surface was prepared by mixing curing agent and base by the proportion of 1 : 40 and pour into the mold. After

leaving for 3 hr 30 min at 60 C°, the surface was solidified, of which thickness $h = 7.5$ mm, the fraction of contact $\phi = 1$, elastic modulus $E \simeq 0.57$ MPa and viscous coefficient $\mu = 117$ kPa·s. The elastic modulus and viscous coefficient were estimated by fitting the data. The PDMS surface was coated with grease (WD-40) to prevent the adhesive effect. The metallic ball (Tsubaki Nakashima co., ltd., SUJ2) was suspended by the electromagnet of which magnet force is controlled. Once the ball is released from the electromagnet, it starts to free fall and collides with the PDMS surface (Fig. S4, the movie is given as Supplemental Material []). After the contact of surface, it reached to the maximum deformation δ_m then rebound to release from surface again.

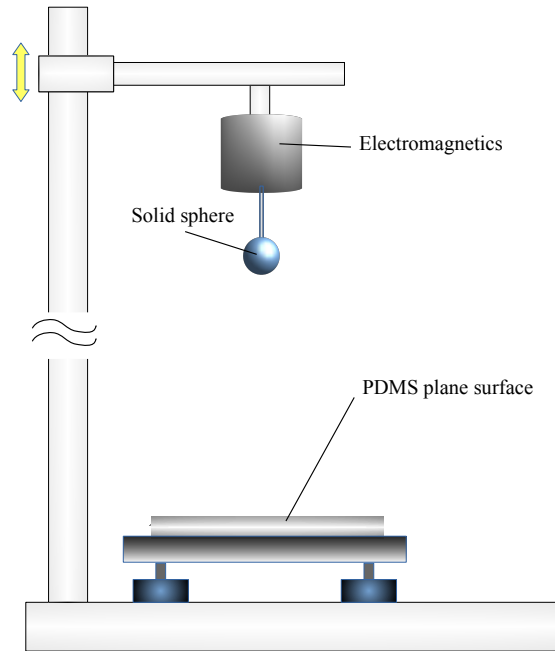


FIG. S3: (Color online) Sketch of experimental setup. The solid sphere is suspended by an electromagnet. The velocity of impact is adjusted by changing the height of the part in which the sphere is suspended. The sphere ($R = 3.0, 4.0, 5.0, 6.0, 7.0$ and 8.0 mm, $\rho = 7800$ kg · m⁻³) is dropped onto the PDMS plane surface ($\phi = 1, h = 7.5$ mm).

The process is observed by high speed camera (FASTCAM SA1.1, 768 × 768 pixel, 10000 fps). The size of sphere R is differed as 3.0, 4.0, 5.0, 6.0, 7.0 and 8.0 mm, of which density $\rho = 7800$ kg · m⁻³. The collision experiments were performed for 6 times in each conditions. The information of velocity, maximum deformation, contact time and so on were extracted from the movies by image analysis which is programmed by Python using Open CV.

In my model, I utilized the scaling relation $t_c \sim \delta_m/v_i$ [13]. According to the experimental results, the coefficient between t_c and δ_m/v_i is estimated to be : $t_c = 1.90\delta_m/v_i$. Therefore, we have the following conversion between De and Z as $1/De \simeq 1.90 Z$ (Fig. S5).

-
- [1] G. I. Barenblatt, *Scaling* (Cambridge University Press, 2003) pp.60-65.
 - [2] G. I. Barenblatt, *Scaling, self-similarity, and intermediate asymptotics* (Cambridge University Press, 1996) pp.86-94.
 - [3] G. I. Barenblatt, *Flow, Deformation and Fracture* (Cambridge University Press, 2014).
 - [4] G. I. Barenblatt and Ya. B. Zeldovich, Self-similar solutions as intermediate asymptotics, *Ann. Rev. Fluid Mech.* **4**, 285 (1972).
 - [5] See Refs. [1] (pp. 91-93), [2] (pp.159-160).
 - [6] See Refs. [1] (pp.82-91), [2] (pp.151-159) and [3] (pp. 153-163).
 - [7] Ya. B. Zeldovich, The motion of a gas under the action of short term pressure shock. *Sov. Phys. Acoustics*, **2**, 25 (1956).
 - [8] See Refs. [1] Ch.3 and [2] Ch.3, 4.
 - [9] N. Goldenfeld, *Lecture On Phase Transitions And The Renormalization Group* (Addison-Wesley Publishing Company, 1992) Ch.10.

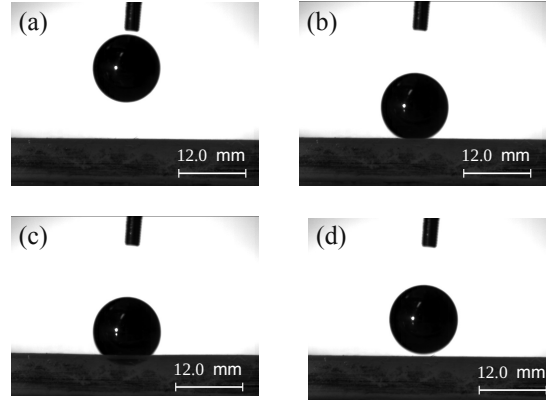


FIG. S4: (Color online) The images of the dynamical impact of sphere ($R = 6.0$ mm) onto the elastic surface at $v_i = 370$ mm/s with the frame rate for 10000 images per second and the resolution of 768×768 pixels. (a) The image before impact. (b) The moment of contact. (c) The moment of maximum deformation at $t = 11$ ms after contact. (d) The image releasing from surface after contact. The movie is uploaded as Supplemental Material [].

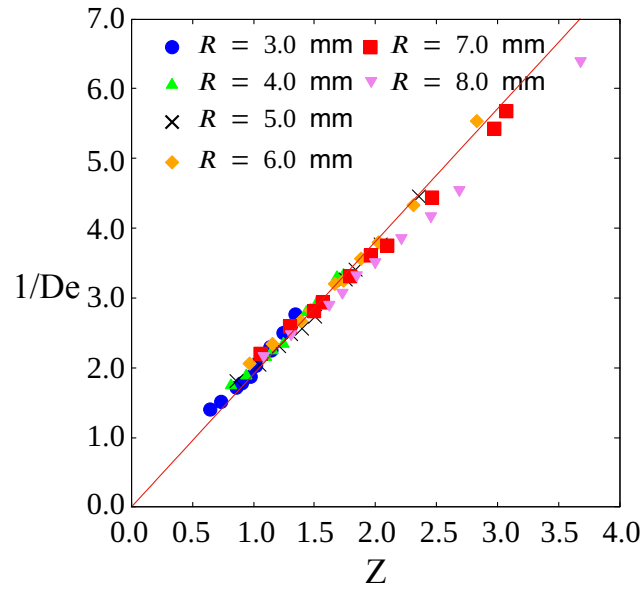


FIG. S5: (Color online) The plots between Z and $1/De$ in which $Z = \frac{E\delta_m}{\mu v_i}$ and $De = \frac{\mu}{Et_c}$. The red line indicates the slope $\simeq 1.90$.

- [10] N. Goldenfeld, O. Martin and Y. Oono, Intermediate asymptotics and renormalization group theory, *J. Sci. Comput.* **4**, 355 (1989).
- [11] G. I. Barenblatt and L. R. Botvina, Incomplete similarity of fatigue in a linear range of crack growth, *Fatigue Eng. Mater. Struct.* **3**, 193 (1981).
- [12] M. H. Holmes, *Introduction to Perturbation Methods* (Springer 2nd ed., 2013) pp.22-27.
- [13] K. L. Johnson, *Contact mechanics* (Cambridge University Press, 1985). p. 353.